

## **Instability Line as a Basic Characteristic of Non-Cohesive Soils**

**Waldemar Świdziński, Jacek Mierczyński**

Institute of Hydro-Engineering, 80-328 Gdańsk-Oliwa, ul. Kościarska 7,  
e-mails: waldek@ibwpan.gda.pl, mier@ibwpan.gda.pl

(Received December 14, 2004; revised March 15, 2005)

### **Abstract**

In the paper, the experimental results of undrained response of non-cohesive soil subjected to either monotonic or cyclic loading, are analysed and discussed. The analysis was based on the results of comprehensive testing programme made of “Skarpa” sand investigated in the triaxial compression. Two main undrained behaviours such as liquefaction and cyclic mobility were experimentally identified and studied. In the analysis of undrained behaviour, the concept of steady state of deformation has been adopted. It was shown that the undrained response of non-cohesive soils is governed by different failure mechanisms than in the case of drained samples. In undrained failure mechanism, an important role is played by an instability line, which may be identified with the initiation of potential liquefaction.

**Key words:** liquefaction, cyclic mobility, instability

### **1. Introduction**

Experimental evidence from tests on several types of soils have clearly indicated that loose saturated non-cohesive soils when subjected to either monotonic or cyclic loading in undrained conditions, may liquefy. In the first case the liquefaction is associated with dramatic drop in shear strength up to residual value, which usually occurs at or slightly after the top of the undrained stress path in deviator – mean effective stress space, far from failure surface, and is followed by a substantial increase of pore water pressure. This process is associated with large deformations which develop when soil liquefies. The liquefaction phenomenon caused by monotonic loading is often referred in the literature, as static liquefaction.

Slightly different behaviour is observed when the same non-cohesive soil, in similar undrained conditions, is subjected to cyclic shearing. In this case, during the substantial part of the loading process, the pore water pressure builds up rather slowly causing respectively slow decrease of effective stresses, with almost

no reduction of shear strength, at very small deformations. However, further continuation of cyclic loading may also lead to such a decrease of effective stresses that the soil can not resist to any shear stress and also liquefies. The number of cycles to trigger liquefaction in a given soil varies usually from several to several hundreds and is a function of its initial state and the magnitude of cyclic shear stress amplitude. The soil liquefaction in this case is identified with zero effective stress, see Seed and Lee (1967). At zero effective stress the soil has very little stiffness or no stiffness at all which also results in large deformations developing during this stage of cyclic loading.

In nature, the liquefaction phenomenon is usually observed in very loose non-cohesive saturated soils. It is related to the tendency of such soils to decrease in volume during shearing when loosely-packed individual soil particles of the soil attempt to move into a denser configuration. The water is “trapped” and prevents the soil particles from moving closer together, that being accompanied by an increase in water pressure which reduces the contact forces between the individual soil particles, thereby softening and weakening the soil deposit. However, in laboratory conditions the liquefaction was also experimentally triggered in very dense sands (Castro 1975). Such soils are of a dilative character, revealing expansion in volume under loading conditions. The number of cycles required to cause liquefaction in such soils may exceed thousands. Another mechanism of pore water generation in denser soils as compared with looser ones, together with some other differences in soil behaviour, which may also finally lead to its liquefaction, was termed as cyclic mobility, originally introduced by Cassagrande, see Green and Ferguson (1971).

These two different phenomena of undrained behaviour of saturated non-cohesive soils are strongly related to its initial state, described however, not only by soil's initial density but also the stress state the soil is subjected to, prior to shearing. In considerations of the above issue it is very useful to imply the concept of steady state of deformation, proposed originally by Castro in his PhD thesis and literally defined by Poulos (1981). According to this concept, there exists a unique line in the void ratio – mean effective stress space, corresponding to steady state of deformation of a soil. The line splits assumed space into two regions representing different soil behaviours. The soils, the state of which can be described by points located above this line, exhibit contractive behaviour i.e. decrease in volume during shearing whereas the soils, the state of which is represented by points located below the steady state line are of dilative character, which means that they expand when sheared. This approach is very useful in understanding the general behaviour of granular materials under loading conditions and particularly in distinguishing two different phenomena related to the undrained response of non-cohesive soils. According to the idea of steady state of deformation, the liquefaction is attributed to the contractive soils and may be triggered by either monotonic or cyclic loading, whereas cyclic mobility is a feature of dilative soils subjected to cyclic loading

(Castro 1975, Castro and Poulos 1977). More detailed considerations on the steady state of deformation will be discussed in the following section of the paper.

According to the definition given by Morris in 1983 (after Sladen et al. 1985), which is also attributed to Castro (Lipiński 2000), "... Liquefaction is a phenomenon wherein a mass of soil loses a high percentage of its shear resistance, when subjected to monotonic, cyclic, or shock loading, and flows in a manner resembling liquid until the shear stresses acting on the mass are as low as reduced shear resistance". Historically, the liquefaction phenomenon was first attributed to the behaviour of a subsoil built of non-cohesive saturated soils, due to earthquakes. It resulted in a great interest of researchers in studying the undrained behaviour of soils under cyclic loading. However, the observed in nature flow slides of underwater artificial islands and hydraulically deposited fills (c.f. Sladen et al. 1985), which took place without the presence of cyclic loading, altered the direction of studies towards the undrained response of saturated non-cohesive soils also to monotonic loading. The pioneering work of such response has been carried out by Castro and summarized in his PhD thesis. In Poland, very comprehensive experimental studies on the undrained response of cohesionless soils with various contents of fines, subjected to monotonic loading were being performed by Lipiński (2000).

During monotonic undrained loading of loose sands, sudden reduction of shear strength to a constant residual value is followed by reaching the peak resistance. This means that the behaviour of soil may become unstable before failure, understood in the classical manner, and the region of potential instability is located inside failure surface, e.g. according to Coulomb-Mohr failure criterion. Subsequently, in the case of cyclic undrained response of such sand the liquefaction condition identified with zero effective stress may be reached only in the origin of stress space. This, in turn, means that there must also exist a certain threshold being a border of instability region in the stress space, similar to the region observed in the case of static liquefaction. Such a threshold may be identified with the initiation of liquefaction before failure surface or zero effective stresses are reached. According to Yammamuro and Lade (1997), soil instability is a phenomenon that resembles liquefaction in that there is a sudden decrease in the soil strength under undrained conditions, which is associated with the development of large pore pressures that reduce the effective stresses in the soil. This loss of strength can occur well inside the effective stress failure envelope.

The paper is simply devoted to experimental studies of the instability problem in the process of liquefaction of saturated non-cohesive soils, in both monotonic as well as cyclic undrained soil response cases and to clarify its role for initiation of liquefaction phenomenon, as well as for general behaviour of non-cohesive soils. The main inspiration of the research programme has resulted from a need to correctly explain the predictions of compaction/liquefaction model developed in the Institute, related to the cyclic undrained behaviour of saturated non-cohesive

soils, directly prior to liquefaction which, in the model, is also identified with zero effective stress.

All tests have been performed in the triaxial apparatus manufactured by GDS Ltd. Company, in the geomechanical laboratory of the Institute of Hydro-Engineering, IBW PAN. The results show that there exists a single line in a stress space, located inside the failure surface, being the border, the achievement of which can be identified with the initiation of liquefaction in both monotonic and cyclic load conditions, in the case of undrained response or with the qualitative change of that response in drained soils.

## 2. Concept of Steady State of Deformation

The concept of steady state of deformation for sands originated from Casagrande's idea of "critical void ratio", (Green and Fergusson 1971) and extended later by critical state concept, proposed by Schofield and Wroth, 1968 for clays as well. It was Castro who first termed the ultimate constant state the sample of loose sand reaches during monotonic triaxial shearing in undrained conditions, after rapid drop of shear strength from peak shear resistance to the residual value, as the steady state (Lipiński 2000). On the basis of Castro's extensive experimental work, Poulos (1981) defined the steady state of deformation for any mass of particles as the state in which the mass is continuously deforming at constant volume, constant normal effective stress, constant shear stress and constant velocity. The steady state is achieved only after orientation of all particles has reached a statically steady-state condition and after all particle breakage, if any, is complete, so that the shear stress needed to continue deformation and its velocity remains constant. Such state corresponds to residual constant shear strength which in this case, is identified with liquefaction of the soil. The term "steady state" is used to reflect the steady-state flow of liquefied sand, whereas the term "deformation" is used to emphasize that the steady state exists only when deformation is ongoing (Poulos 1981).

Steady state of deformation is described by two parameters: void ratio and mean effective stress during steady state. The pairs of these values corresponding to steady state, when plotted in the void ratio – mean effective stress space (presented in semi-logarithmic scale  $e - \log p'$ ), are located along the common line designated as steady state line.

Typical steady state line has been schematically shown in Fig. 1. It can be noticed that the value of mean effective stress may change completely the behaviour of any granular material which e.g. when in dense state and subjected to sufficiently high pressures may behave similarly to loose material. Additionally, the steady state line may be treated as a reference level with respect to which initial

state of soil is evaluated. The evaluation is expressed by the so called state parameter defined as the void ratio difference between the initial sand state and the steady state conditions at the same mean effective stress (Been and Jefferies 1985).

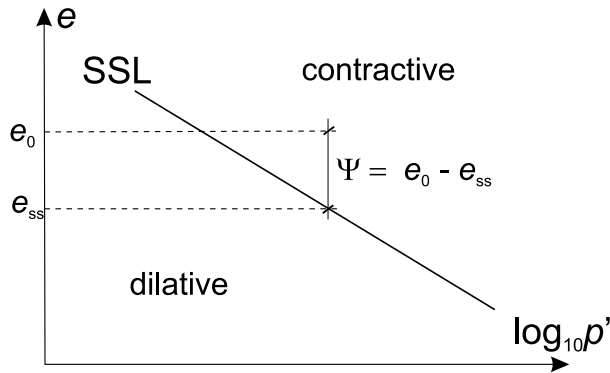


Fig. 1. Typical shape of steady state line

In order to explain better the above considerations, let us consider a loose sandy sample which has been fully saturated and next monotonically loaded in a triaxial compression test, under undrained conditions in a strain controlled mode. Typical response of such a sample is presented in Fig. 2.

The results of the test have been interpreted in terms of stress deviator –  $q$ , mean effective stress –  $p'$ , pore water pressure –  $u$  versus axial strain –  $\varepsilon_z$  and  $q$ ,  $p'$  stress space, where  $q = \sigma_1 - \sigma_3$ ,  $p' = (\sigma_1 + 2\sigma_3)/3$ , accordingly.

In the first stage of loading (Fig. 2a), the increase of stress deviator to its maximum value is observed, accompanied by an increase of pore water pressure causing respective decrease of mean effective stress, according to Terzaghi's fundamental rule  $p' = p - u$ .

In this particular case, the peak shear resistance equal to 140 kPa was reached at 1% of axial strain, after which a sudden decrease of shear stress, that at 10% of axial strain achieved only 40 kPa was observed and remained constant during further shearing process, up to 27% of axial deformation. According to Poulos's definition, the state of the sample characterized by its behaviour within the range of 10 to 27% of axial strain corresponds to steady state of deformation and respective residual mean effective stress –  $p'_{res}$ , together with initial void ratio  $e_0$  which remains constant in undrained conditions, represent the steady state points lying on the steady state line.

### 3. Instability of the Soil

When analysing the undrained response in terms of stress path, Fig. 2b, one should note that the peak resistance is not associated with the Coulomb-Mohr failure envelope and cannot be referred to failure. Further loading after passing

the peak shear resistance causes a decrease of stress deviator associated with an increase of strains. The reduction of shear stress lasts until the residual value at steady state is reached. The increase in strain at decreasing load is typical of unstable behaviour of the material. This means that in the case of undrained response of loose non-cohesive soils, the condition of maximum stress deviator does not correspond to the true failure condition, but rather to a condition of minimum stress difference at which instability may develop inside the true failure surface (Lade 1992). The condition corresponding to failure in undrained response is usually represented by maximum effective principal stress ratio ( $\sigma'_1/\sigma'_3$ ) and occurs after the maximum stress deviator is reached. Thus, these two conditions i.e. maximum stress deviator and maximum effective principal stress ratio designate the region of potential instability, being the upper and lower bounds of the region, respectively. According to Sladen et al. (1985, see also Lade 1992, 1994) instability is a state where the shear stress reaches a maximum inside the true failure surface and then decreases. It will be further shown that, although the instability is not synonymous with failure, both may lead to catastrophic events.

The initiation of unstable behaviour after passing the peak shear stress suggests that there exists a line in the stress space corresponding to the lower bound of instability region and separating potentially unstable stress states from stable ones. Such a line is called the instability line (see Lade 1992), being the locus of instability states for one initial density and varying confining pressures.

The term 'potential instability' has been used due to the fact that the undrained response may not always lead to final failure which in this case is equivalent to liquefaction. According to Castro (after Konrad 1990, see also Lipiński 2000) three main types of the undrained response can be observed i.e. strain softening (SS), limited strain softening (LSS) and strain hardening (SH), Fig. 3. The first two are both strain softening responses and may finally lead to liquefaction and/or partial or limited liquefaction, respectively.

Typical strain softening response is presented in Fig. 2. In turn, in LSS type there is a transition stage, corresponding to minimum shear resistance after which the increase of stress is observed. This minimum strength, in LSS undrained response type, may temporarily achieve such residual values which may lead to partial or limited liquefaction. Subsequently, strain hardening response (SH) represents a path in the stress space in which the sand will exhibit a strain hardening behaviour that will not lead to liquefaction. Such state is attributed to highly dilative soils.

#### **4. Experimental Programme and Testing Procedures**

##### *Aim of the experimental work*

The general aim of experimental work was to study the undrained response of saturated non-cohesive soils to monotonic and cyclic loadings. In particular, the

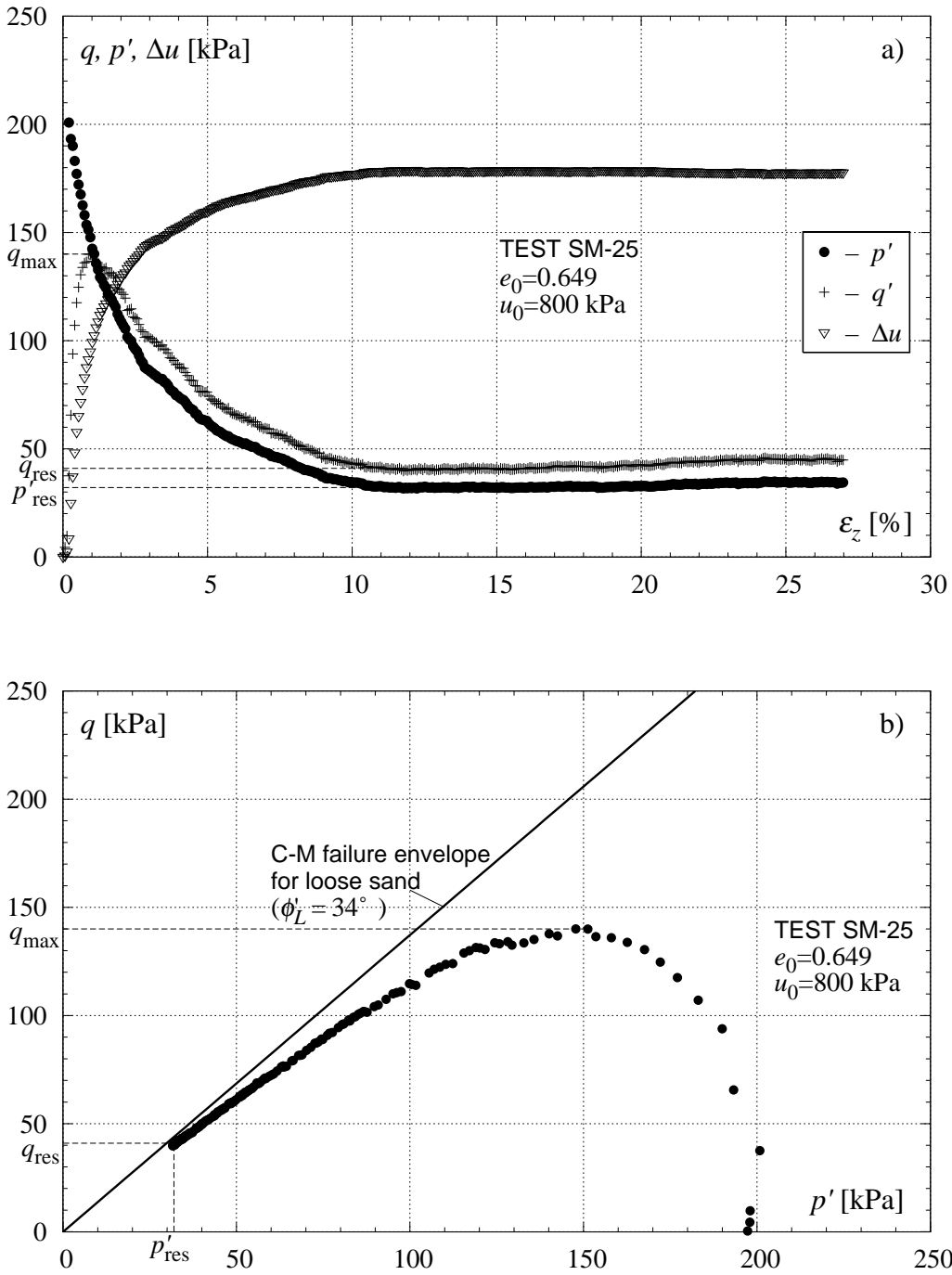


**Fig. 2.** Typical results of undrained triaxial compression test of loose "Skarpa" sand;  
 a) stress deviator, mean effective stress and pore water pressure versus axial strain,  
 b) stress path in  $q, p'$  stress space

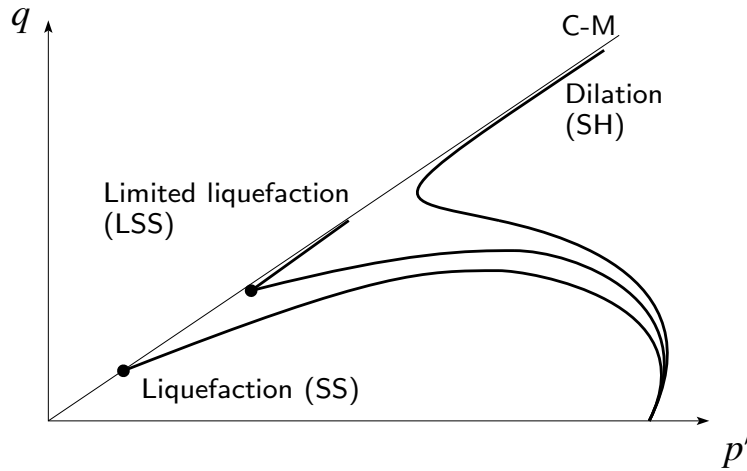


**Fig. 3.** Various types of undrained response of non-cohesive soils to monotonic loading

work was focused on the pronounced verification of a steady state concept for sands, its role in the assessment of liquefaction susceptibility of granular materials, different undrained responses to monotonic and cyclic loadings depending on the initial state of the soil tested, the conditions of initiation of liquefaction and particularly the role of instability line in failure process.

The majority of tests was performed on saturated samples, however, some tests on dry samples were also carried out.

#### *Sand tested*

All tests in the present study were performed on a sand which for practical purposes has been named “Skarpa”. The sand is composed principally of quartz and can be classified as subangular medium sand with a median grain size of approximately  $420 \mu\text{m}$  and uniformity coefficient of 2.5. The specific gravity is 2.65. “Skarpa” sand has a maximum void ratio of 0.677 and minimum void ratio of 0.432. The angles of internal friction for loose ( $I_D = 0.15$ ) and dense sand ( $I_D = 0.87$ ) are  $34^\circ$  and  $41^\circ$ , respectively.

#### *Equipment used*

All tests have been carried out using a fully computer controlled triaxial testing system manufactured by GDS Instruments Ltd. Company. The system consists of a triaxial cell of the Bishop and Wesley type with internal load cell, housing specimens of 38 mm in diameter and 80 mm in height, digital pressure-volume controllers for controlling cell and back pressures, as well as axial load, and data acquisition system linked to desktop computer. The volume change (in drained tests) or the pore-water pressure (in undrained tests) of the sample was measured



by one of the controllers, which can either control back pressure while measuring volume change, or control volume change while measuring pore-water pressure. In this study the tests were performed in both strain and load controlled modes, including cyclic loading.

A single test consisted of four main stages: preparation of the specimen to the desired density, saturation to the required value of  $B$  Skempton's coefficient playing with back pressure, consolidation to the presumed confining pressure and final loading, according to the procedures described by Poulos (1981, see also Been and Jefferies 1985, Lipiński 2000).

### *Specimen preparation*

All samples were prepared in a membrane-lined split mould either by moist tamping (MC) or by water pluviation (PL) methods. The first method assured an achievement of relatively uniform, very loose samples which revealed contractive behaviour when sheared, whereas the second one, uniformity of denser samples exhibiting dilative character. The split mould was attached to the lower platen of the cell and the membrane held to the inside of the mould by vacuum.

In the case of moist compacted samples five pre-weighted portions of sand were mixed with de-aired water to give about a 3 to 5% water content. Each portion of sand was then compacted into the mould to a predetermined height corresponding to the desired void ratio. Wet pluviated samples were prepared from the sand which was also first mixed with de-aired water and then spooned into the mould filled initially with 30% of de-aired water. The mould was tapped gently to densify the sample if necessary, to obtain the required weight of soil in the mould.

Once the sample was in the mould and closed by the top platen, a vacuum pressure of the order of 15 kPa was applied. It allowed easy assembling of the triaxial cell or gauges for local measurement of horizontal and radial strains to control the void ratio change during saturation and consolidation stages, without disturbance of the sample and preserving the initial void ratio, particularly in very loose samples. After assembling the triaxial cell and filling it with de-aired water the vacuum pressure was then replaced by the same confining pressure.

### *Saturation*

In next stage of the tests (for moist tamping method) the specimens were saturated in two phases. In the first phase, carbon dioxide was slowly flushing through the specimen under low pressure in order to remove air from the voids and replace it by the gas dissolving in water. This ensured more complete saturation. This phase lasted from 1 to 2 hours. The sample was next saturated with de-aired water at an average rate of  $100 \text{ mm}^3/\text{min}$ . After the end of this process the degree of saturation was checked and corrected by increasing the back pressure until  $B$

value of at least 0.97 was achieved. The back pressures which were applied to fulfill full saturation condition ranged from 500 to 800 kPa.

### *Consolidation*

The samples were next isotropically consolidated to the desired effective pressures equal to  $p'_c = 100, 200, 400$  and  $800$  kPa, respectively. The average rate of consolidation was set at max. 10 kPa/min.

### *Testing programme*

The testing programme has been summarized in Table 1. Within the frame of the experimental programme two main types of tests were carried out, namely: monotonic compression triaxial (MT) and cyclic triaxial tests (CT) for various initial states of the specimens and loading conditions. Test conditions varied considerably and included drained (5) and undrained (29) conditions for 22 specimens prepared by moist compaction method and 2 by wet pluviation.

## **5. Monotonic Undrained Response**

In order to study the undrained response to monotonic loading of the sand tested the steady state line has been first determined. To do that both undrained as well as drained tests have been carried out for various initial states of the sand (various initial void ratios and mean effective stresses), see Table 1. The samples were sheared in strain controlled mode at a strain rate varying from 10 to 12 mm/h. All monotonic tests were being conducted up to the end of range of the piston's vertical movement which corresponded to approximately 30% of vertical strain of the sample tested. In the case of undrained conditions (zero volume change), during shearing axial load and pore water pressure versus axial strain were monitored (at confining pressure kept constant). In drained tests the volume change of the sample was measured either directly by local gauges installed on it or by measuring the volume of water sucked or expelled from the sample during shearing. The details can be found in Świdziński and Mierczyński (2002 and 2003).

According to the previous considerations discussed at the end of Section 2, stress paths presented correspond to three main responses of saturated non-cohesive soil subjected to monotonic loading in undrained conditions. Typical strain softening response (SS) has already been presented in Fig. 2. Such behaviour is characteristic for the soil, which when subjected to large strains reaches a steady state of deformation. The second type of the undrained response is represented by the results of test No. SM-34, presented in Fig. 4 where shear strength drops after peak strength to the minimum value and then increases slightly (limiting liquefaction softening behaviour – LLS).

And finally the third type of undrained response corresponds to the stress path represented by the result of test No. SM-28, Fig. 5 in which after little softening, essential hardening (SH) of the sample is observed. This hardening is accompanied with simultaneous decrease of pore-water pressure which in the case of drained sample corresponds to increase in volume.

Stress paths for all undrained monotonic tests carried out within the framework of the assumed testing programme have been collected in Fig. 6.

Completely different response is observed in the case of drained tests. Typical results of such a test have been shown in Fig. 7. In the test, the sample of saturated "Skarpa" sand has been first consolidated to the confining pressure of 100 kPa and then sheared (test No. SM-17).

When analyzing the results shown in Fig. 7 it can be seen that in the first stage of loading the sample compacts slightly and then significantly dilates. The dilation begins at approximately 1% of axial strain, far prior to achievement of maximum strength. This is opposite to the behaviour observed in the case of undrained response of the soil. After reaching peak strength, the sample softens slightly to the ultimate value at very large strains. The softening is accompanied by further dilation which tries to reach asymptotic value, as well. In the case of tests described in this paper the full achievement of ultimate volumetric strain (no further volume changes) was not possible due to constraints of the triaxial

apparatus used in the experiments. However, it can be assumed that in the case of the test the results of which are presented in Fig. 7, at the end of the test, the sample was approaching steady state of deformation and void ratio and mean effective stress corresponding to the final stage of shearing represent a point lying on steady state line.

In Fig. 8 the results of all monotonic tests, representing steady state of deformation have been plotted in void ratio – mean effective stress space. Points denoted by full dots correspond to steady state of deformation of saturated samples in undrained tests whereas open circles represent a steady state of deformation obtained from drained tests. The points have next been approximated by a straight line, in the form proposed by Been and Jefferies (1985):

$$e = e_{ss} - b \log(p'), \quad (1)$$

where  $e_{ss}$  represents void ratio corresponding to steady state at 1 kPa mean effective stress and  $b$  a declination of the steady state line. In the case of "Skarpa" sand the values were 0.746 and 0.0635, respectively (see Świdziński and Mierczyński 2003).

All types of soil undrained response shown in Fig. 6 reveal one common feature i.e. unstable behaviour manifesting by a descending response at increasing vertical strain just after passing the peak stress. When the condition of instability

**Table 1.** Summary of testing programme

Initial conditions					Test conditions				End of test		
Test No.	Preparation	Void ratio $e_0$	$I_D$	$p'_c$ [kPa]	Drainage	Loading	$\Delta q$ [kPa]	$q_{avr}$ [kPa]	$q_{max}$ [kPa]	$q_{res}$ [kPa]	$N_f$
SM-17	WP	0.537	0.571	100	D	MT	–	–	310*	250	–
SM-18	WP	0.510	0.682	400	D	MT	–	–	1100*	1000	–
SM-21	MC	0.581	0.392	200	D	MT	–	–	480	–	–
SM-23	MC	0.606	0.290	50	D	MT	–	–	130	–	–
SM-24	MC	0.622	0.224	25	D	MT	–	–	70	–	–
SM-25	MC	0.649	0.114	200	U	MT	–	–	140	41	–
SM-30	MC	0.640	0.151	400	U	MT	–	–	230	87	–
SM-33	MC	0.592	0.347	800	U	MT	–	–	580	342	–
SM-34	MC	0.595	0.335	800	U	MT	–	–	500	277	–
SM-35	MC	0.628	0.200	400	U	MT	–	–	270	97	–
SM-36	MC	0.624	0.216	400	U	MT	–	–	280	101	–
SC-3	MC	0.645	0.131	200	U	CT	60	60	–	–	4
SC-6	MC	0.645	0.131	200	U	CT	28	60	–	–	146
SC-7	MC	0.643	0.139	200	U	CT	37	60	–	–	37
SC-8	MC	0.636	0.167	200	U	CT	48	60	–	–	13
SC-10	MC	0.654	0.094	200	U	CT	18	60	–	–	438
SC-14	MC	0.647	0.122	200	U	CT	27	60	–	–	123
SC-16	MC	0.650	0.110	100	U	CT	18.7	30	–	–	1–2
SC-17	MC	0.650	0.110	100	U	CT	26	30	–	–	10
SC-18	MC	0.660	0.069	100	U	CT	13.3	30	–	–	55
SC-27	MC	0.647	0.122	200	U	CT	32	60	–	–	97
SC-30	MC	0.653	0.098	200	U	CT	43	60	–	–	38
SC-31	MC	0.590	0.355	200	U	CT	40	60	–	–	330**
SC-32	MC	0.582	0.388	200	U	CT	50	60	–	–	220**

MC – moist compacted, WP – wet pluviated, U – undrained, D – drained, MT – monotonic triaxial tests, CT – cyclic triaxial tests, \* – no clear peak,

\*\* – large strain amplitudes without essential shear strength reduction

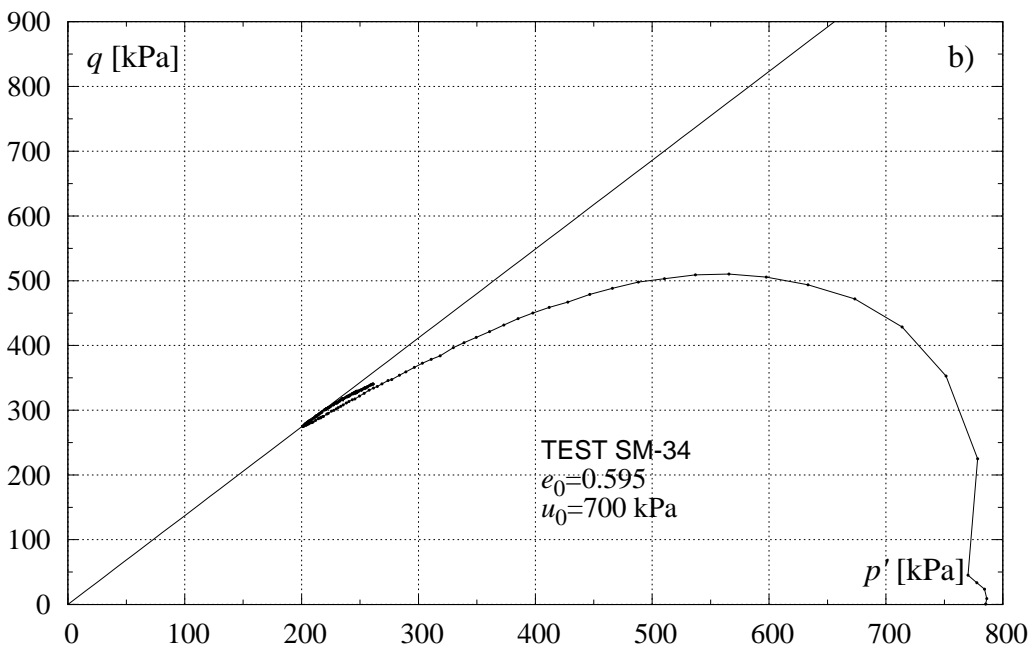
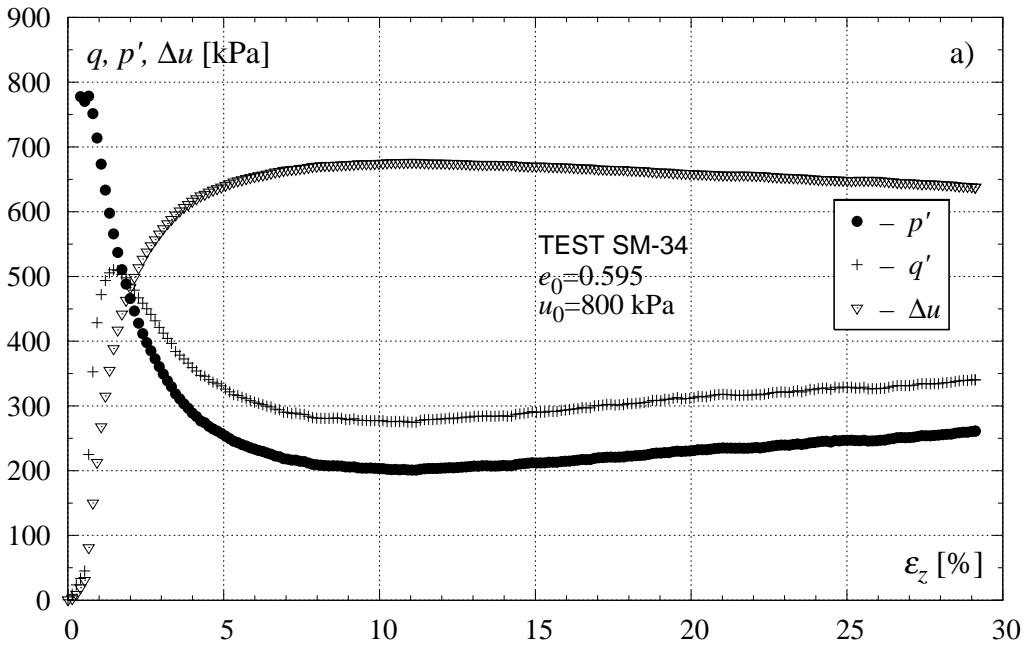


Fig. 4. An example of LSS (limited strain softening) undrained response

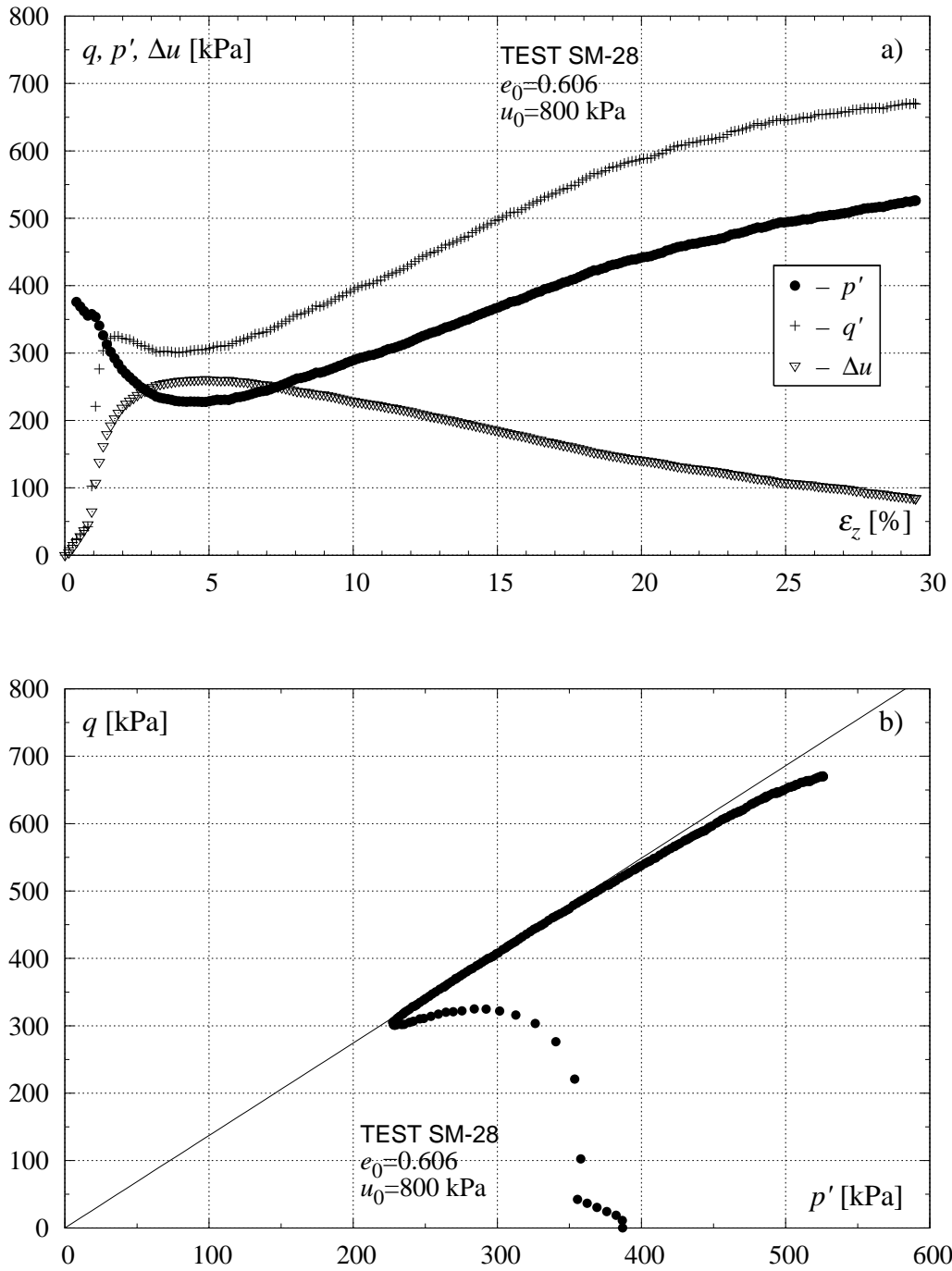


Fig. 5. Strain hardening (SH) undrained response of "Skarpa" sand

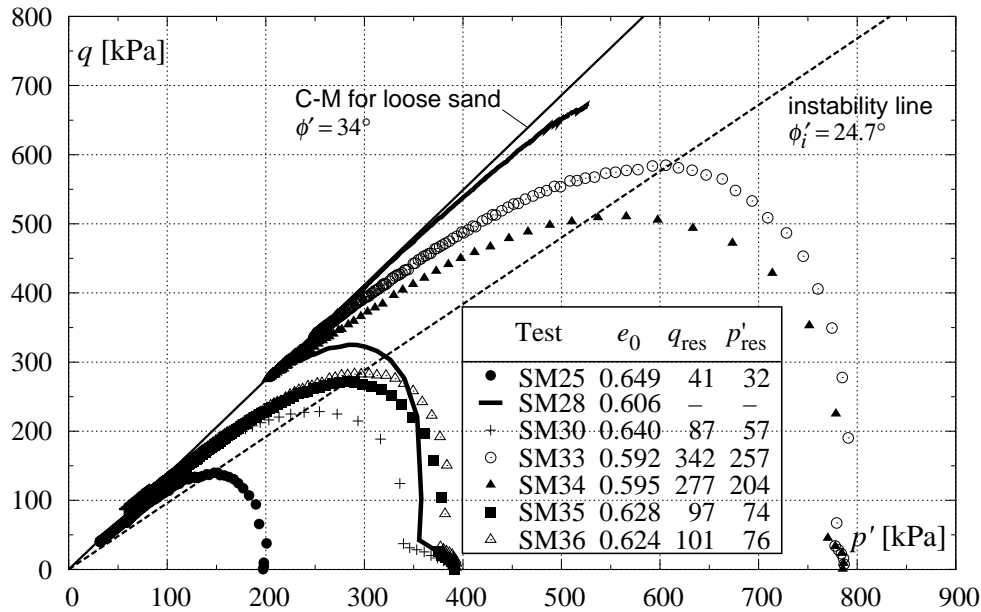


Fig. 6. Stress paths from various undrained triaxial compression tests of “Skarpa” sand for various initial void ratios and various consolidation and back pressures

is reached, the soil may not be able to sustain the current stress state. This stress state corresponds to the top of the undrained effective stress paths expressed by stress deviator. Thus, the line connecting the tops of a series of effective stress paths from undrained tests on loose soil provides the lower limit of the region of potential instability (Lade 1992).

It can be seen from the results of undrained tests presented in Fig. 6 that the points corresponding to peak stress can be nicely approximated by straight line which passes the origin. In fact, this line should pass through the steady state point which is characterized by residual strength, however, for extremely loose sands this residual strength is very low and for practical purposes the line goes through the origin of the stress space.

It should also be noted that in all tests discussed, the peak stress occurred and approximately 1% of axial strain, the same value at which dilation was being initiated in the case of drained tests (see Figs. 2a, 4a and 7a).

The instability line is a lower limit of the region of potential instability whereas the upper limit is defined by the failure line determined from drained tests. In the case of “Skarpa” sand the slope of instability line is equal to  $q_{peak}/p' = 0.97$  which corresponds to the angle  $\phi'_i = 24.7^\circ$  at the angle of internal friction of loose drained sand  $\phi'_L = 34^\circ$ . These values are close to those obtained by other authors.

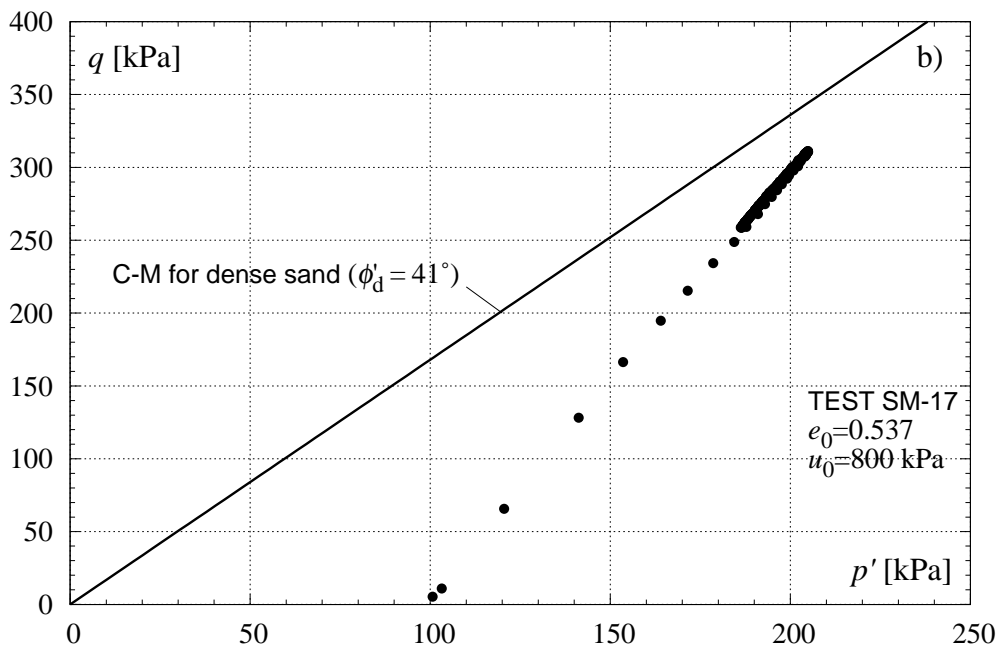
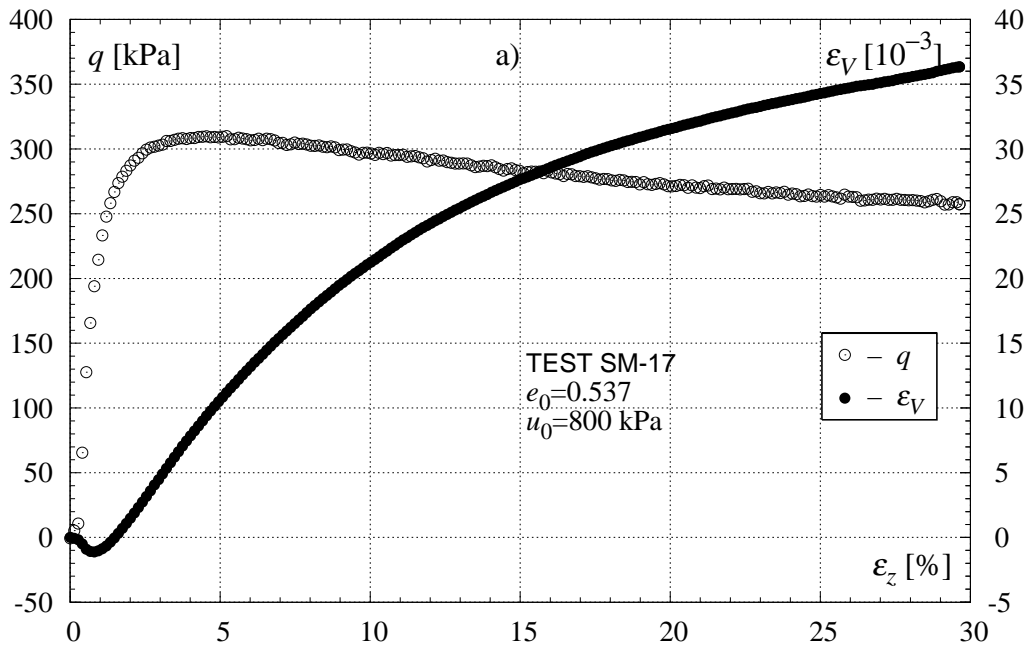


**Fig. 7.** Typical results of monotonic drained triaxial compression test for dense “Skarpa” sand;  
 (a) – stress deviator and volumetric strain versus vertical strain,  
 (b) – stress path in the  $q - p'$  stress space



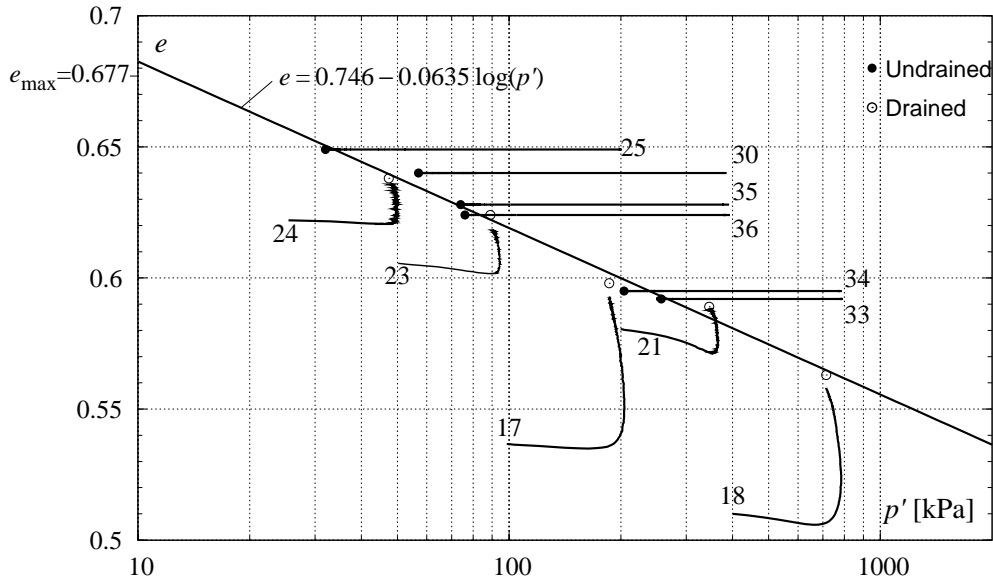


Fig. 8. Steady state line for „Skarpa” sand

Based on large series of experiments performed on various non-cohesive soils with various fine contents Lipiński (2000) suggests the universal criterion corresponding to the condition of instability defined by effective deviatoric stress  $q$  to be equal to mean effective stress  $p'$ , which can be written as:

$$\frac{q}{p'} = 1, \quad \text{or} \quad \frac{\sigma'_1}{\sigma'_3} = 2.5 \quad (2)$$

In fact, the value obtained for “Skarpa” sand is very close to that proposed by Lipiński although it is hard to find any physical explanation of this condition. Furthermore, Lipiński suggests that the instability criterion can play the role of necessary condition to trigger liquefaction. The last conclusion seems, in turn, to be reasonable. When we analyse the development of pore-water pressure during undrained tests performed on loose sand (Fig. 2a) we can easily see that at the peak stress, over 60% of the final value of pore-water pressure corresponding to liquefaction, was generated. Thus, such a suggestion is experimentally justified. It will be better seen in the case of undrained response of soil subjected to cyclic loading.

## 6. Cyclic Undrained Response

In cyclic triaxial compression tests the sample was first consolidated to the desired confining pressure  $p'_c$  and then slightly loaded to the assumed average stress deviator  $q_{avr}$  just to have reference level for cyclic loading above the hydrostatic line. In order to study the influence of the confining pressure on the number of loading cycles to trigger liquefaction, the cyclic tests were carried out for two values of  $p'_c = 100$  and 200 kPa and corresponding average stress deviator  $q_{avr} = 30$  and 60 kPa, respectively. Independently, the tests were made for two main initial soil states: contractive and dilative and different stress amplitudes varying from 13.3 to 60 kPa, see Table 1. Initial states of cyclically sheared specimens, referring to steady state line for the sand tested, have been plotted in the  $e - \log p'$  space and shown in Fig. 9.

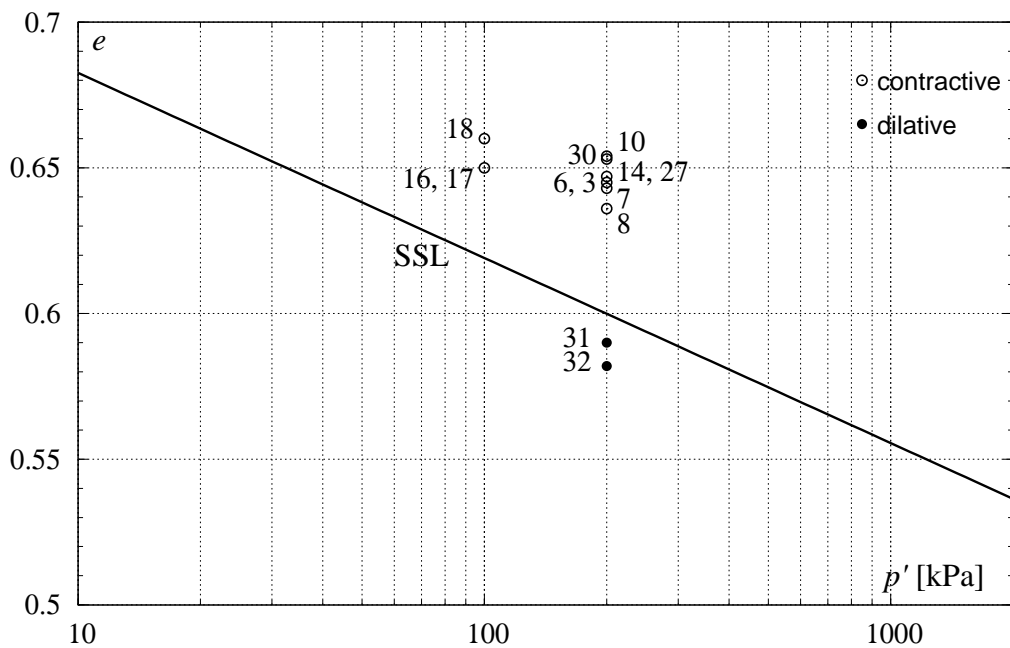


**Fig. 9.** The initial states of specimens of “Skarpa” sand subjected to cyclic triaxial loading in  $e - \log p'$

During the test, pore-water pressure, as well as axial deformation, were measured in a function of loading cycles. Due to constraints of the triaxial system used, the period of a single loading cycle was rather long varying from 1 minute to 2 minutes. In the case of cyclic loading the tests were carried out under stress controlled conditions.

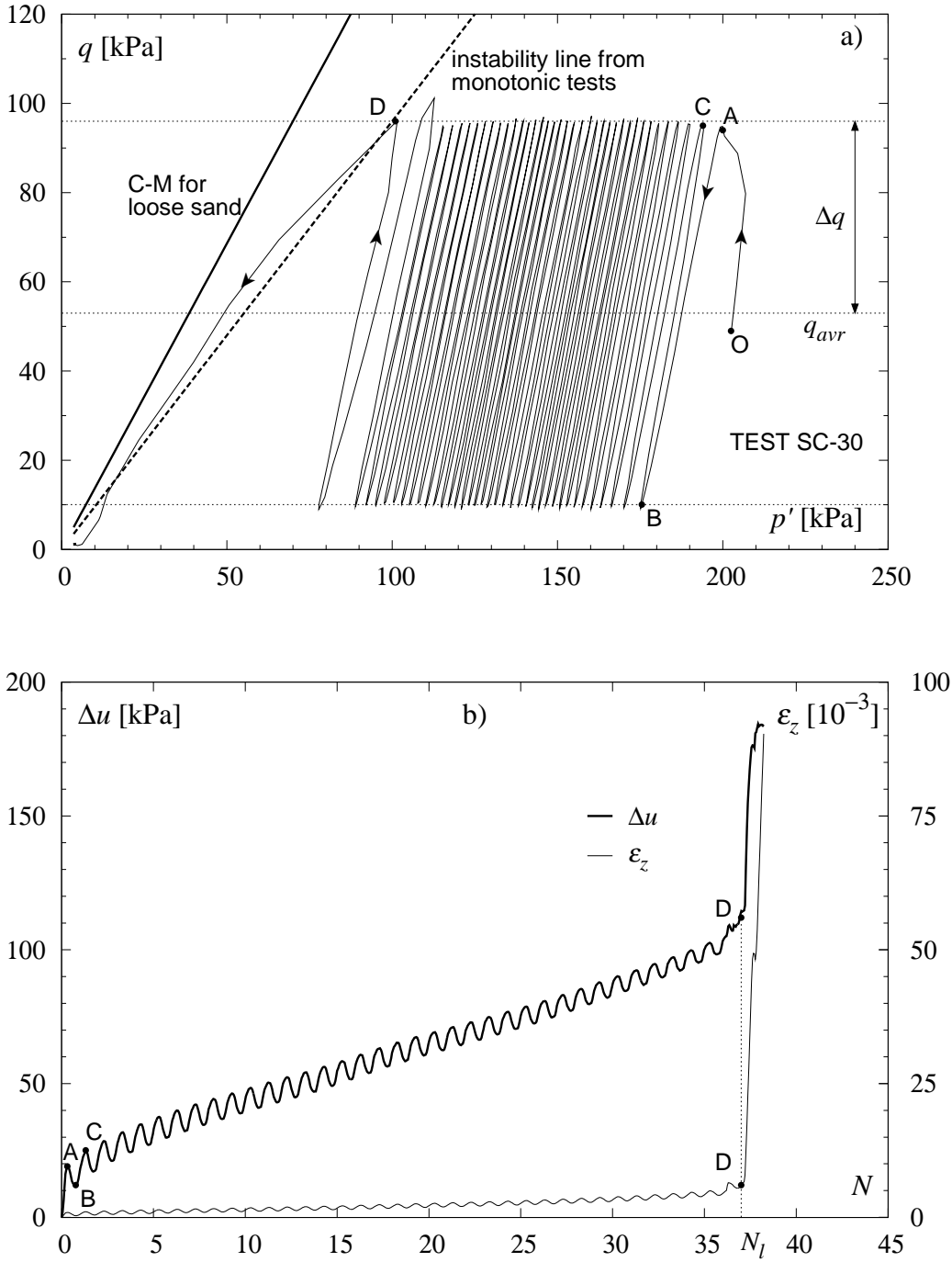
Typical results of cyclic compression tests for contractive samples, corresponding to the test No. SC-30 are shown in Fig. 10. In this test the sample was first isotropically consolidated to the confining pressure  $p'_c = 200$  kPa and then loaded to the assumed stress deviator of 60 kPa which was the reference level for subsequent cyclic loading. Practically, the actual average deviatoric stress was 53 kPa. Then the sample was subjected to cyclic shearing with the amplitude of  $\pm 43$  kPa around the reference level. The shape of cyclic loading wave was very close to sinusoidal form.

Fig. 10a shows the realization of cyclic triaxial compression test in stress space whereas in Fig. 10b the response expressed in terms of pore-water pressure generation and the change of axial strain with the number of loading cycles.

It can be seen that subsequent cycles of loading cause cumulative increase of pore pressure with no change of shear strength. The average trend of pore-water pressure is almost linear with small regular oscillations around, being a response to cyclic loading waves. The increase of pore-water pressure causes, in turn, consequent decrease of effective stresses which results in the movement of the stress path towards the classical failure surface. Respective increase of axial strains during this phase which covers a substantial part of the whole test is very small and does not exceed 1%.

In cycle 38 of loading, rapid increase of pore-water pressure was observed, which was accompanied with a sudden drop in shear strength to zero effective stress and large increase of axial strain up to complete collapse of the specimen. Such behaviour is typical for liquefaction phenomenon. The liquefaction started when the stress path, being at its highest point resulting from assumed average stress deviator and stress amplitude, intersected the instability line at point D, see Fig. 10a. Note that the instability line plotted in Fig. 10a, in the form of a dashed line, has been determined based on monotonic undrained triaxial tests. It is also seen that Coulomb-Mohr failure surface determined from drained tests does not directly play any role in undrained failure which occurs inside it. In addition, it should be noted that the start of liquefaction took again place at 1% axial strain, the same value at which qualitative changes were observed in monotonic response for both undrained and drained tests.

Slightly different behaviour is observed in the case of cyclically sheared dilative samples, however, dilative tendency is not too considerable in this case, see Fig. 9. The results of the cyclic triaxial test on such a sample are presented in Fig. 11. In this case, after the stress path intersects the instability line there is no shear strength reduction as observed for contractive samples, but stabilization of the stress path in the form of a closed hysteresis loop which during loading phase is tangent to Coulomb-Mohr failure envelope. In this stage of the test, during each subsequent cycle, the strains become progressively larger, as more cycles of load are applied, see Fig. 11b. Such behaviour can be identified with the onset of "partial liquefaction" or "initial liquefaction" (Castro 1975). According to



**Fig. 10.** Typical results of cyclic triaxial compression test made on contractive sample; a) stress space, b) generation of pore-water pressure and changes of axial strain versus number of loading cycles

Castro, when the strain reaches the value of 20%, the sand is said to have attained “complete” liquefaction. Such a state can be identified with strain softening failure which differs significantly from that observed in the case of contractive samples.

In Fig. 12, normalised shear stress amplitude versus number of loading cycles to cause liquefaction for two levels of effective confining stress for contractive samples are shown. The points were approximated by exponential functions. The results presented in Fig. 12 are in qualitative agreement with those obtained by other authors (Martin et al. 1975, Sawicki 1991). According to these, the number of cyclic loading to cause liquefaction increases with the decrease of stress amplitude and increased effective confining stress. The later conclusion is the opposite of that observed in undrained response to monotonic loading where the samples with a given initial void ratio when sheared under higher confining pressures are more contractive and thus more susceptible to liquefaction. This was one of basic reasons for which Casagrande (Green and Ferguson 1971), in order to differentiate the behaviours of undrained response to monotonic and cyclic loading, introduced for the later the term “cyclic mobility”, although many authors refer this term to the cyclic undrained response of dilative samples only.

Cyclic mobility can be induced in the laboratory even on the densest sand and the resistance to cyclic mobility at a given void ratio also increases with increasing confining pressure, where the resistance to cyclic loading is expressed as the cyclic deviator stress needed to produce a certain strain in a given number of cycles (Castro 1975).

## 7. Discussion

In Fig. 13, the points corresponding to the beginning of instable behaviour for both monotonic as well as cyclic undrained tests are plotted in the  $q - p'$  stress space. In the case of monotonic response the points are equivalent to peak stress values and corresponding mean effective stresses in each test (see Fig. 6) whereas for cyclic triaxial tests the highest value of cyclic stress path prior to failure (equivalent to point D from Fig. 11), after passing which the stress paths drop to zero effective stress. It can be seen that all the points can be approximated with high accuracy by a single straight line being the instability line for the sand tested. This line bounds the region inside which the sand may reveal instable character in undrained conditions, that consequently may lead to its liquefaction.

According to Lade (1993), because sands are perfectly stable above the instability line as long as they are drained, the instability line itself is in principle not a trigger mechanism for an instability. However, this line also plays an important role in the case of drained conditions splitting the stress space onto two regions in which the soil, when subjected to shearing, exhibits different qualitative behaviour, which was schematically shown in Fig. 14. In the lower region, below the instability line, the non-cohesive soil reveals a contractive character and

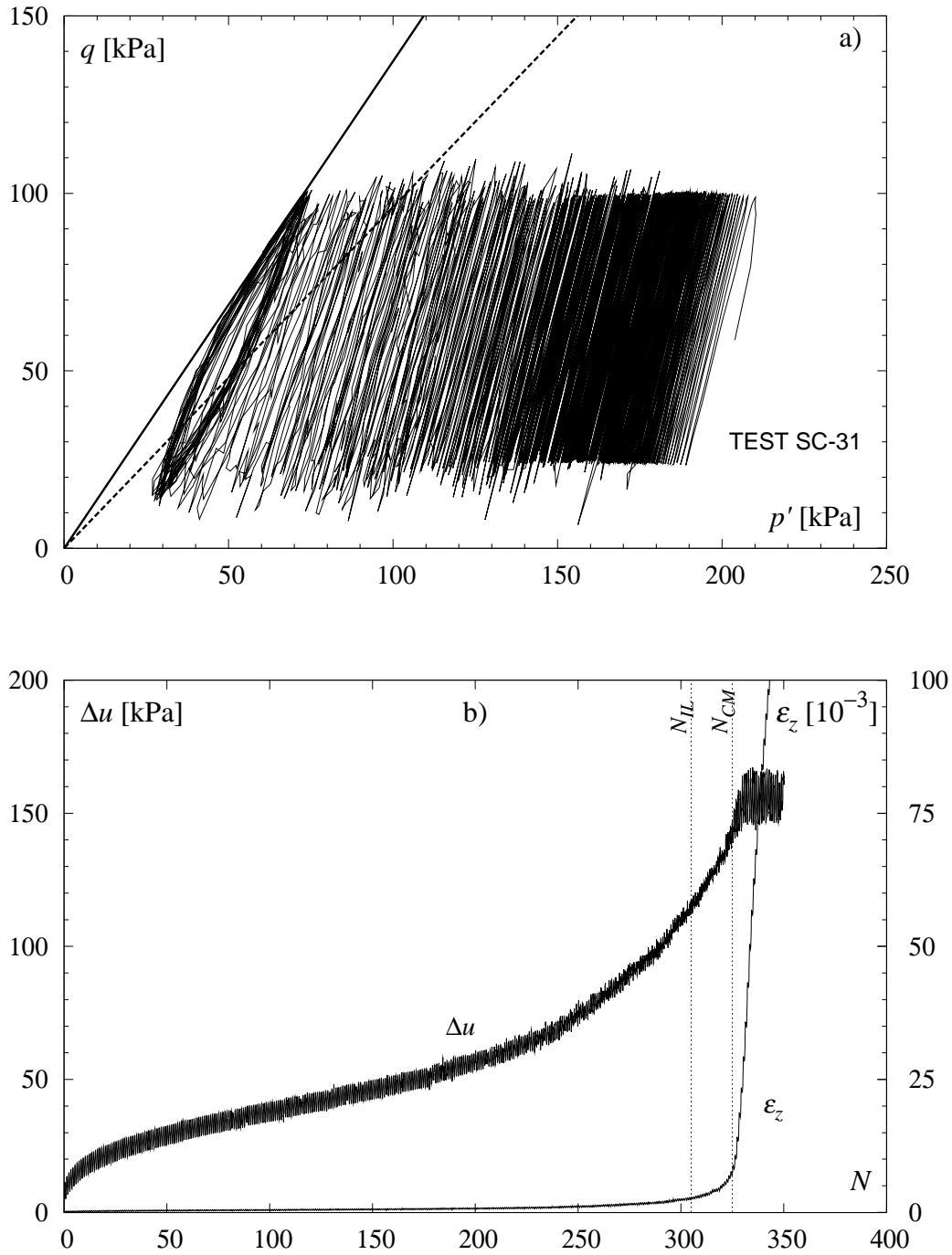


**Fig. 11.** Typical results of a cyclic triaxial compression test made on a dilative sample; a) stress space, b) generation of pore-water pressure and changes of axial strain versus number of loading cycles

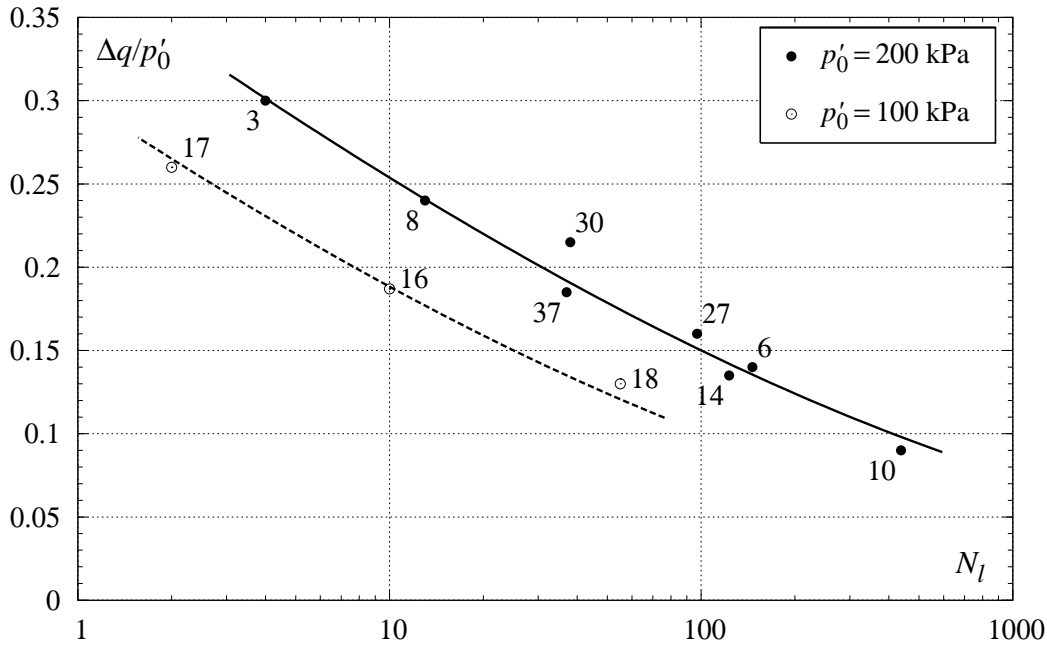


**Fig. 12.** Normalized amplitude of stress deviator versus number of cycles to cause liquefaction for two levels of effective confining pressure

compacts during shearing, whereas after passing the instability line, in the upper region, the soil dilates. The presence of such a line for dry sands was identified in previous works of the authors, during studies on the development of pre-failure strains of granular materials in the triaxial test (see Sawicki and Świdziński 2003).

A common feature of all tests carried out during these studies was the fact that regardless of the types of loading and loading conditions, qualitative change in the soil's response has been observed at approximately the same level of axial load i.e.  $\sim 1\%$ , (compare Figs. 2a, 4a, 5a and 7a). It confirms the existence of such a line in the stress space.

In the case of undrained behaviour, the instability line is a lower bound of the instability region. The upper bound is defined by the drained failure line according to Coulomb-Mohr yield condition. For granular material to become unstable, the state of stress must be located on or above the instability line. In the region above the instability line, the soil can deform to large magnitudes of strain under decreasing stresses. In the case of loose non-cohesive soils instability leads to liquefaction caused by sudden decrease in the soil strength under undrained conditions. This loss of strength is related to the development of large pore-water pressures that reduce the effective stresses in the soil.

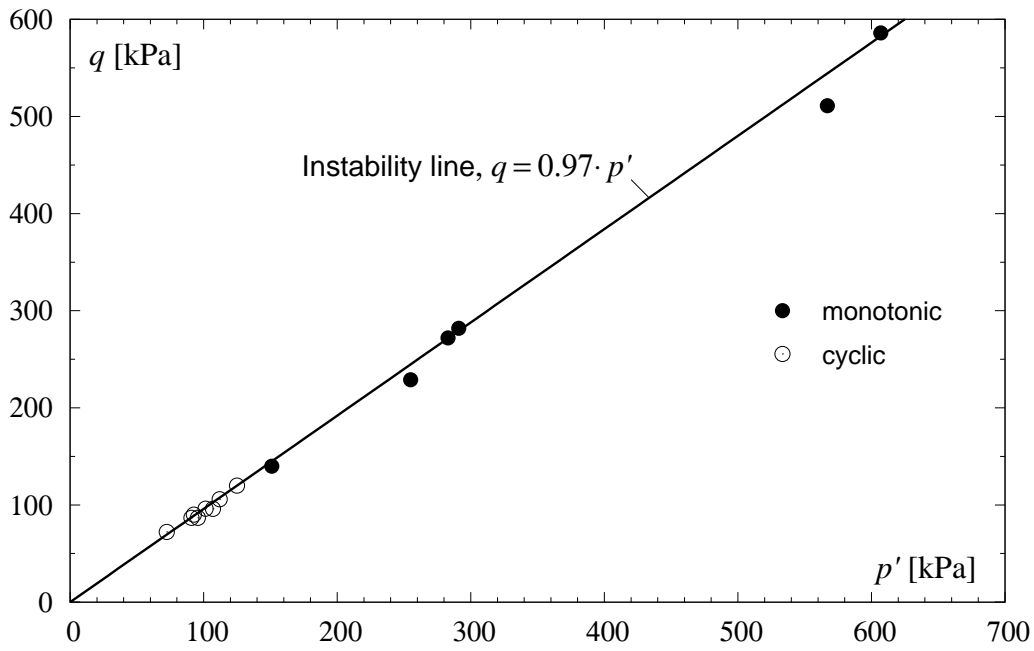


**Fig. 13.** Instability line of "Skarpa" sand determined from monotonic and cyclic triaxial undrained tests

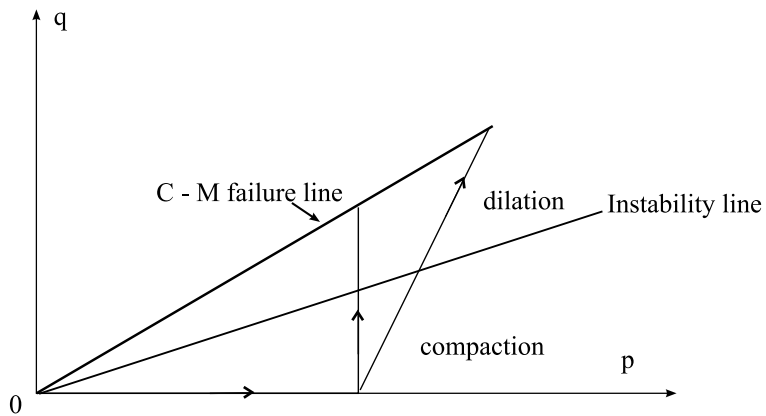


**Fig. 14.** Compaction and dilatation zones during shearing of dry sand



Based on the experimental results shown in this paper, as well as considerations presented here, it is clear that the condition of maximum stress difference does not correspond to true failure conditions, but rather to conditions of minimum stress difference in which instability may develop inside the true failure surface, and the loss of strength in the case of undrained monotonic response can occur well inside the failure envelope (see also Lade 1992).

The stress conditions, the soil has at instability line, can be identified with initial liquefaction which may, but not necessarily, lead to complete or final liquefaction defined by zero effective stress. In the second case the soil behaviour is characterized by a temporary drop in load shear strength caused by rising pore pressure, however, continued shearing results in recovery of shear strength due to conditions which allow the soil to dilate after initial instability. Such behaviour is defined by Lade (1993) as temporary instability and the line at which the soil re-gains its strength is defined by Ishihara et al. (1975) as a phase transformation line.

In practice, soil instability and subsequent liquefaction may mostly occur in loose soils, however, it should be noted that according to the steady state of deformation concept, dense sands can also become unstable if the confining pressures are sufficiently high.

The above considerations justify the conclusion that besides the failure line corresponding to drained shear resistance, the instability line is a second basic characteristic governing the behaviour of sheared non-cohesive soils and deserves further detailed experimental and theoretical studies.

## 8. Summary

Two main behaviours of saturated non-cohesive soil subjected to monotonic and cyclic loading in undrained conditions are discussed and experimentally confirmed i.e. liquefaction and cyclic mobility. Liquefaction and cyclic mobility have in common the development of high pore pressures at constant volume which, in both cases, may lead to failure however of different nature. Liquefaction consists of a loss in shear strength and can only occur in non-cohesive soils that are looser than the critical state defined by a steady state line, whereas cyclic mobility consists of gradually increasing cyclic strains and can occur in both loose as well as dense soils, but does not trigger a loss in shear strength. Another significant difference between these two phenomena is the dependence of confining pressure. In the case of loose sands of a given void ratio, subjected to monotonic loading in undrained conditions the susceptibility to liquefaction increases with the increase of confining pressure, whereas in cyclic mobility phenomena the increase of confining pressure increases the resistance to liquefaction.

A common feature of both phenomena is the fact that in both cases there exists a unique line in the stress space at which the initiation of liquefaction may occur.

The instability line is lower bound of instability region within which saturated non-cohesive soils in undrained conditions may exhibit instable behaviour, i.e. can produce large strains under decreasing stresses. The upper bound of the instability region is determined by a drained failure line. In the case of “Skarpa” sand tested in the frame of studies presented, the drained failure line, for the Coulomb-Mohr failure criterion adopted, is characterised by the angle of internal friction for loose sand equal to  $34^\circ$  whereas the corresponding angle of instability line in equivalent stress space was  $24^\circ$ .

In the case of drained samples the instability line splits the stress space onto two regions in which below the instability line the non-cohesive soil reveals a contractive character and compacts during shearing and above it, the soil dilates, increasing in volume.

Based on the large series of monotonic and cyclic triaxial tests carried out on the sand in various state conditions it has been experimentally proved that the instability line may play a very important role in the behaviour of non-cohesive soils and be a failure criterion in the case of undrained conditions. This concept, however, as well as the attempt of theoretical description of the ideas presented in this paper require further detailed studies.

### References

- Been K., Jefferies M. G. (1985), A State Parameter for Sands, *Geotechnique*, 35, No. 2, 99–112.
- Castro G. (1975), Liquefaction and Cyclic Mobility of Saturated Sands, *J. Geotech. Engrg. ASCE*, Vol. 101, No. GT6, 551–569.
- Castro G., Poulos S. J. (1977), Factors Affecting Liquefaction and Cyclic Mobility, *J. Geotech. Engrg. ASCE*, Vol. 103, No. GT6, 501–516.
- Green P. A., Ferguson P. A. S. (1971), On Liquefaction Phenomena, by Professor A. Casagrande: Report of Lecture, *Geotechnique*, XXI, 3, 197–202.
- Ishihara K., Tatsuoka F., Yasuda S. (1975), Undrained Deformation and Liquefaction of Sand under Cyclic Stresses, *Soils and Foundations*, Vol. 15, No. 1, 29–45.
- Konrad J. K. (1990), Minimum Undrained Strength Versus Steady State Strength of Sands, *J. Geotech. Engrg. ASCE*, Vol. 116, No. 6, June, 948–963.
- Lade P. V. (1992), Static Instability and Liquefaction of Loose Fine Sandy Slopes, *J. Geotech. Engrg. ASCE*, Vol. 118, No. 1, 51–70.
- Lade P. V. (1993), Initiation of Static Instability in the Submarine Nerlerk Berm, *Can. Geotech. J.*, 30, 895–904.
- Lade P. V. (1994), Creep Effects on Static and Cyclic Instability of Granular Soils, *J. Geotech. Engrg. ASCE*, Vol. 120, No. 2, 404–419.
- Lipiński M. J. (2000), *Undrained Response of Cohesionless Soils to Monotonic Loadings*, PhD thesis, Faculty of Hydro and Environmental Engineering, Gdańsk Technical University.
- Martin G. R., Finn W. D. I., Seed H. B. (1975), Fundamentals of Liquefaction under Cyclic Loading, *Proc. ASCE, J. Geotech. ENGN Div.*, 101 (GT5), 423–438.
- Poulos S. J. (1981), The Steady State of Deformation, *J. Geotech. Engrg. ASCE*, Vol. 107, No. GT5, 501–516.
- Sawicki A. (1991), *Soil Mechanics for Cyclic Loadings*, IBW PAN, Gdańsk (in Polish).

- Sawicki A., Świdziński W. (2003), Strain Characteristics of Non-cohesive Soil Subjected to Triaxial Compression *Inżynieria Morska i Geotechnika*, 3/4, 148–152 (in Polish).
- Schofield A., Wroth C. (1968), *Critical State Soil Mechanics*, McGraw-Hill, London.
- Sladen J. A., D'Hollander R. D., Krahn J. (1985), The Liquefaction of Sands, a Collapse Surface Approach, *Can. Geotech. J.*, 22, 564–578.
- Sladen J. A., Handford G. (1987), A Potential Systematic Error in Laboratory Testing of Very Loose Sands, *Can. Geotech. J.*, 24, 462–466.
- Świdziński W., Mierczyński J. (2002), On the Measurement of Strains in the Triaxial Test, *Arch. of Hydro-Engineering and Environ. Mech.*, Vol. 49, No. 1, 23–41.
- Świdziński W., Mierczyński J. (2003), Determination of Steady State Line for Sands, *Inżynieria Morska i Geotechnika*, 3/4, 194–199 (in Polish).
- Yamamoto J. A., Lade P. V. (1997), Static Liquefaction of Very Loose Sands, *Can. Geotech. J.*, 34, 905–917.